Ultrastructural study of spermiogenesis and the spermatozoon in *Catenotaenia pusilla*, an intestinal parasite of *Mus musculus*

C. Hidalgo[1], J. Miquel[1]*, J. Torres[1] and B. Marchand[2]

[1]Laboratori de Parasitologia, Facultat de Farmàcia,
Universitat de Barcelona, Av. Joan XXIII s/n, E08028 Barcelona, Spain:
[2]Département d'Écologie Évolutive, Laboratoire Arago,
Université Pierre et Marie Curie (Paris 6), CNRS UMR 7628, B.P. 44,
F66651 Banyuls-sur-Mer Cedex, France

Abstract

The ultrastructure of spermiogenesis and the mature spermatozoon in *Catenotaenia pusilla* (Cestoda: Catenotaeniidae) is described. Spermiogenesis is characterized by the presence of a single axoneme which grows on the outside of a cytoplasmic extension at an angle of 45°. Flagellar rotation and proximodistal fusion are produced in this process. The centrioles lack striated roots and an intercentriolar body. In the mature spermatozoon four different regions are described. The anterior extremity is capped by an apical cone and presents two helical crest-like bodies of unequal length. The axoneme, of the 9 + '1' pattern of the Trepaxonemata, presents a periaxonemal sheath. The cortical microtubules form a spiral pattern at an angle of about 40° to the hypothetical spermatozoon axis. The nucleus is kidney- to horseshoe-shaped in cross section. Granules and proteinaceus walls are not observed in the spermatozoon of *C. pusilla*.

Introduction

Present knowledge of the ultrastructure of spermiogenesis and/or the spermatozoon in cestodes is limited to 60 species (see Bâ & Marchand, 1995, 1998; Justine, 1995, 1998; Miquel *et al.*, 1999; Sène *et al.*, 1999). Most of these belong to the Cyclophyllidea and in the case of the family Catenotaeniidae, ultrastructural studies on the spermatozoon refer only to two species belonging to two subfamilies: *Catenotaenia pusilla* (Goeze, 1782) (Catenotaeniinae Spasskii, 1950) and *Skrjabinotaenia lobata* (Baer, 1925) (Skrjabinotaeniinae Genov & Tenora, 1979) (Swiderski, 1970; Miquel *et al.*, 1997).

In a previous study, Swiderski (1970) compared spermatogenesis in three cyclophyllidean cestodes: *Catenotaenia pusilla* (Catenotaeniidae), *Inermicapsifer madagascariensis* (Anoplocephalidae) and *Hymenolepis microstoma* (Hymenolepididae). Swiderski's study consisted of a short paper, minus illustrations, delivered at a congress but which offered only an incomplete description of ultrastructural features found in the sperm development of these species. Our work consists of a complete study of spermiogenesis and the spermatozoon in *C. pusilla*, a catenotaeniid cestode which parasitizes the small intestine of *Mus musculus*. We attempt to elucidate possible ultrastructural differences between spermatozoa in representatives of the two subfamilies of Catenotaeniidae as in the case of the subfamilies of the Anoplocephalidae (Bâ & Marchand, 1994a; Justine, 1998).

Materials and methods

Adult specimens of *Catenotaenia pusilla* were collected from the small intestine of naturally infected *Mus musculus* Linnaeus, 1758 (Rodentia : Muridae) from the Les Franqueses del Vallès area, Barcelona, Spain and maintained in a solution of 0.9% NaCl. Different portions

* Fax: +34 93 4024504
E-mail: jmiquel@farmacia.far.ub.es

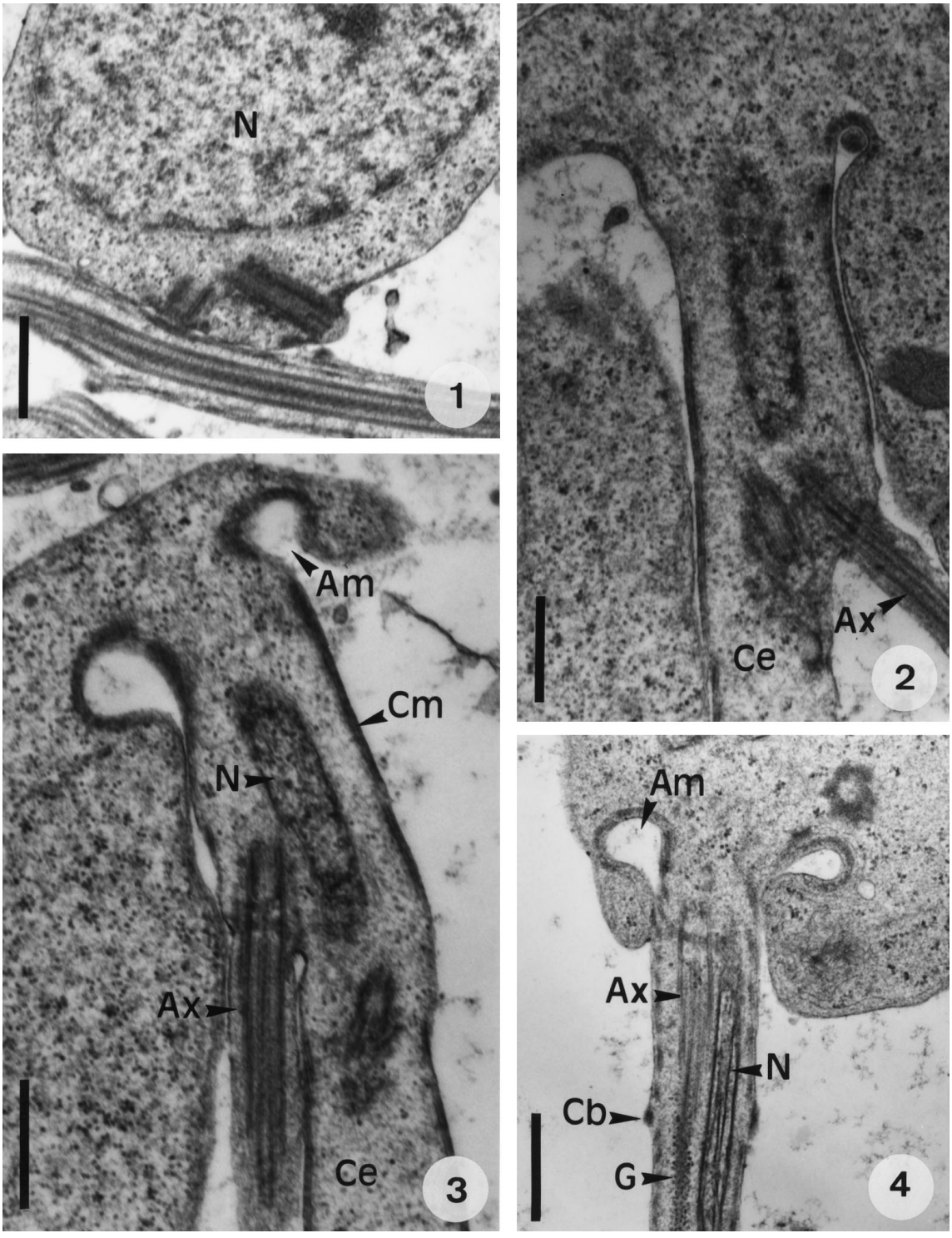

Figs 1–4. Spermiogenesis in *Catenotaenia pusilla*. 1. Differentiating zone showing the nucleus (N) and the disposition of the two centrioles. Bar = 0.5 μm. 2. Longitudinal section of a differentiating zone showing development of the axoneme (Ax) outside the cytoplasmic extension (Ce). Bar = 0.5 μm. 3. Stage of spermiogenesis after flagellar rotation. Am, arched membranes; Ax, axoneme; Ce, cytoplasmic extension; Cm, cortical microtubules; N, nucleus. Bar = 0.5 μm. 4. Longitudinal section of spermatid after proximodistal fusion between the axoneme (Ax) and the cytoplasmic extension. Two crest-like bodies (Cb) appear at the front of spermatid and the nucleus (N) continues to migrate along the spermatic body. Note the presence of granular material (G) around the axoneme. These granules, according to the Thiéry technique, are not glycogen. Am, arched membranes. Bar = 0.5 μm.

of mature proglottids were dissected and fixed in cold 2.5% glutaraldehyde in a 0.1 M sodium cacodylate buffer at 4°C and pH 7.2 for 1 h, rinsed in a 0.1 M sodium cacodylate buffer at 4°C and pH 7.2, postfixed in cold 1% osmium tetroxide in the same buffer for 1 h at 4°C, rinsed in a 0.1 M sodium cacodylate buffer at pH 7.2, dehydrated in ethanol solutions and propylene oxide, embedded in Spurr, and polymerized at 60°C for 48 h. Ultrathin sections were placed on copper grids, and stained with uranyl acetate and lead citrate following Reynolds (1963). The grids were examined in a Hitachi H-600 electron microscope at 75 kV.

The Thiéry (1967) technique was applied for locating glycogen in different spermatid and spermatozoa regions. Gold grids were treated in periodic acid, thiocarbohydrazide and silver proteinate (PA-TCH-SP) as follows: 30 min in 10% of PA, rinsed in distilled water, 24 h in TCH, rinsed in acetic solutions and distilled water, 30 min in 1% SP in the dark, and rinsed in distilled water.

Results

Spermiogenesis

In *C. pusilla*, spermiogenesis begins with the formation of a differentiating zone in the spermatid. This conical area is surrounded by submembranous cortical microtubules and delimited by a ring of arched membranes.

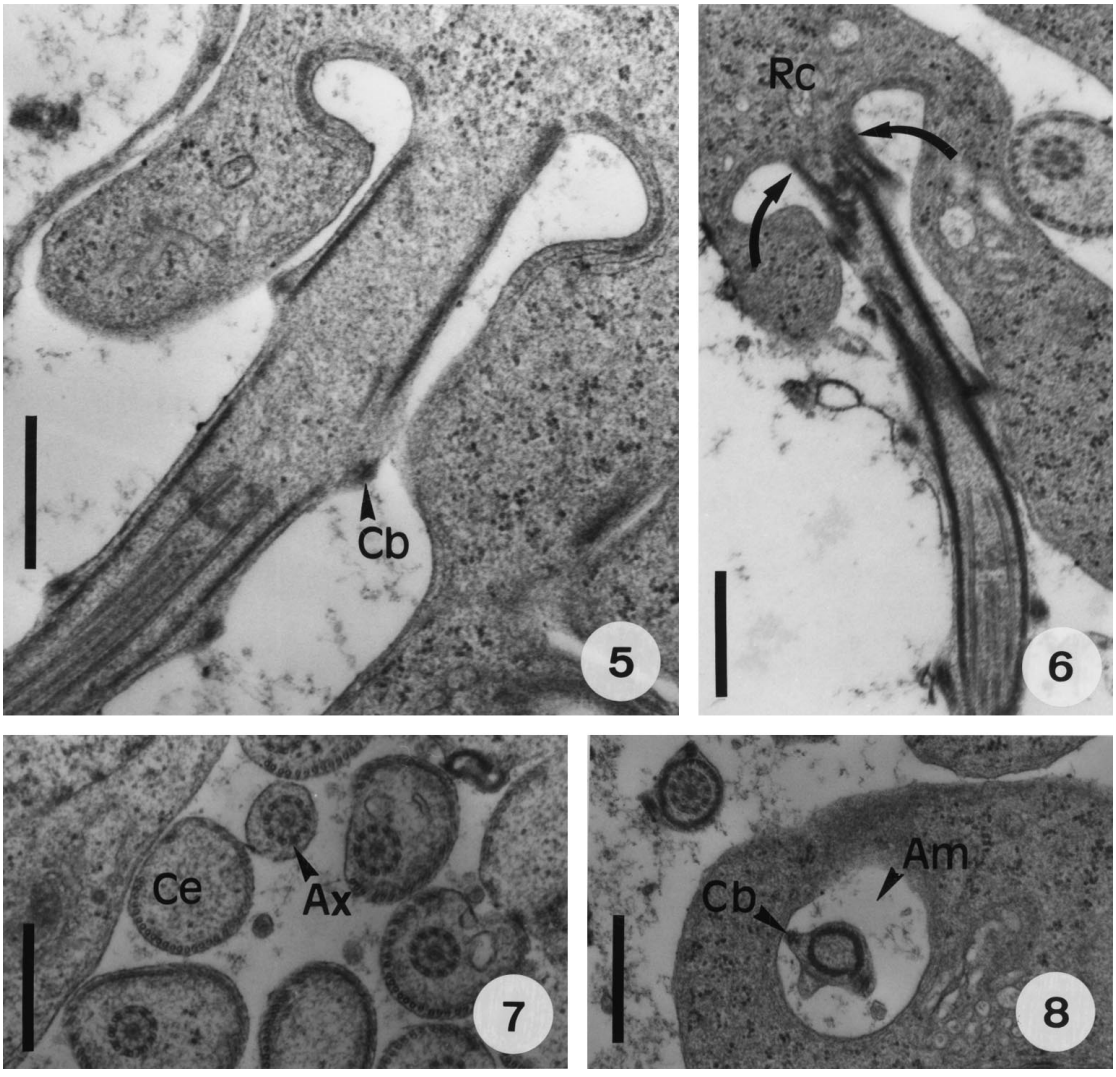

Figs 5–8. Spermiogenesis in *Catenotaenia pusilla*. 5. Spermatid showing two well developed crest-like bodies (Cb). The nucleus has finished its migration. Bar = 0.5 μm. 6. Final stage of spermiogenesis. The strangulation (arrows) of the ring of arched membranes takes place and posteriorly the newly-formed spermatozoon detaches from the residual cytoplasm (Rc). Bar = 0.5 μm. 7. Cross-section of a spermatid after flagellar rotation. Ax, axoneme; Ce, cytoplasmic extension. Bar = 0.5 μm. 8. Cross-section of a spermatid at the level of the ring of arched membranes (Am). Cb, crest-like bodies. Bar = 0.5 μm.

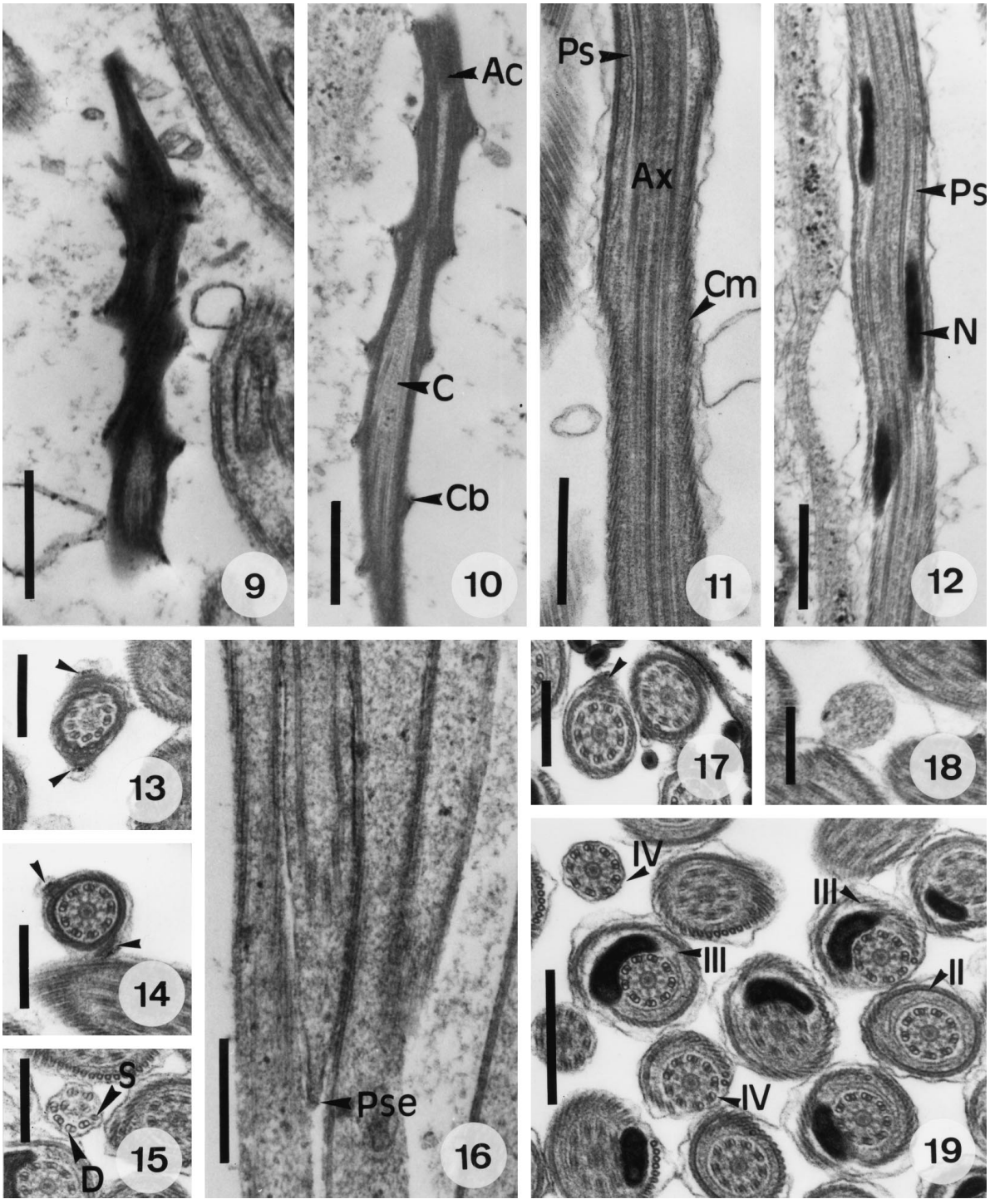

Figs 9–19. Spermatozoon in *Catenotaenia pusilla*. 9. Longitudinal section of the apical cone. Bar = 0.5 μm. 10. Longitudinal section of Region I showing the termination of one crest-like body (Cb) at the level of the centriole (C). Ac, apical cone. Bar = 0.5 μm. 11. Longitudinal section of Region II. Cortical microtubules (Cm) are spiralled at an angle of about 45° to the hypothetical spermatozoon axis. Ax, axoneme; Ps, periaxonemal sheath. Bar = 0.5 μm. 12. Longitudinal section of Region III. N, nucleus; Ps, periaxonemal sheath. Bar = 0.5 μm. 13. Cross-section of Region I at the level of the centriole showing two crest-like bodies (arrow heads). Bar = 0.3 μm. 14. Cross-section of Region I with two crest-like bodies (arrow heads). Bar = 0.3 μm. 15. Cross-section of Region IV showing disorganization of the axoneme. D, doublets; S, singlets. Bar = 0.3 μm. 16. Longitudinal section of Region IV showing the posterior spermatozoon extremity (Pse). Bar = 0.5 μm. 17. Cross-section of Region I with a single crest-like body (arrow head). Bar = 0.3 μm. 18. Cross-section of Region IV following disorganization of the axoneme. Bar = 0.3 μm. 19. Cross-sections of Regions II, III and IV. Bar = 0.5 μm.

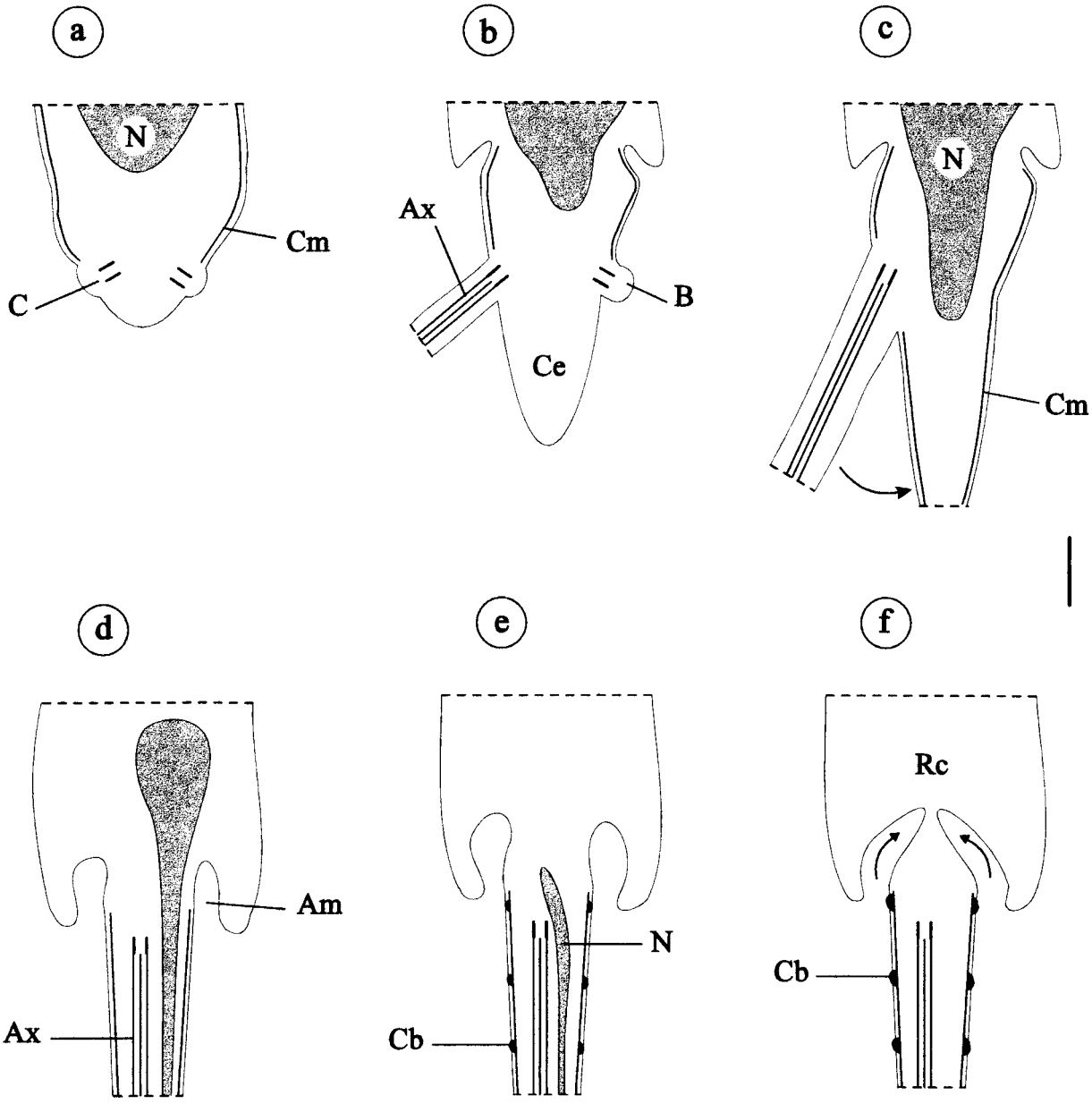

Fig. 20. Reconstruction of the main stages of spermiogenesis in *Catenotaenia pusilla*. a. Zone of differentiation in initial stages of spermiogenesis. C, centriole; Cm, cortical microtubules; N, nucleus. b. The axoneme (Ax) grows outside the cytoplasmic extension (Ce). B, cytoplasmic bud. c. Flagellar rotation (arrow). Cm, cortical microtubules; N, nucleus. d. Proximodistal fusion between the axoneme (Ax) and the cytoplasmic extension. The nucleus initiates its migration along the spermatic body. Am, arched membranes. e. Appearance of crest-like bodies (Cb) at the front of the spermatid. The nucleus (N) continues to migrate. f. Final stage of spermiogenesis. Constriction of the ring of arched membranes (arrows). Cb, crest-like bodies; Rc, residual cytoplasm. Bar = 1 μm.

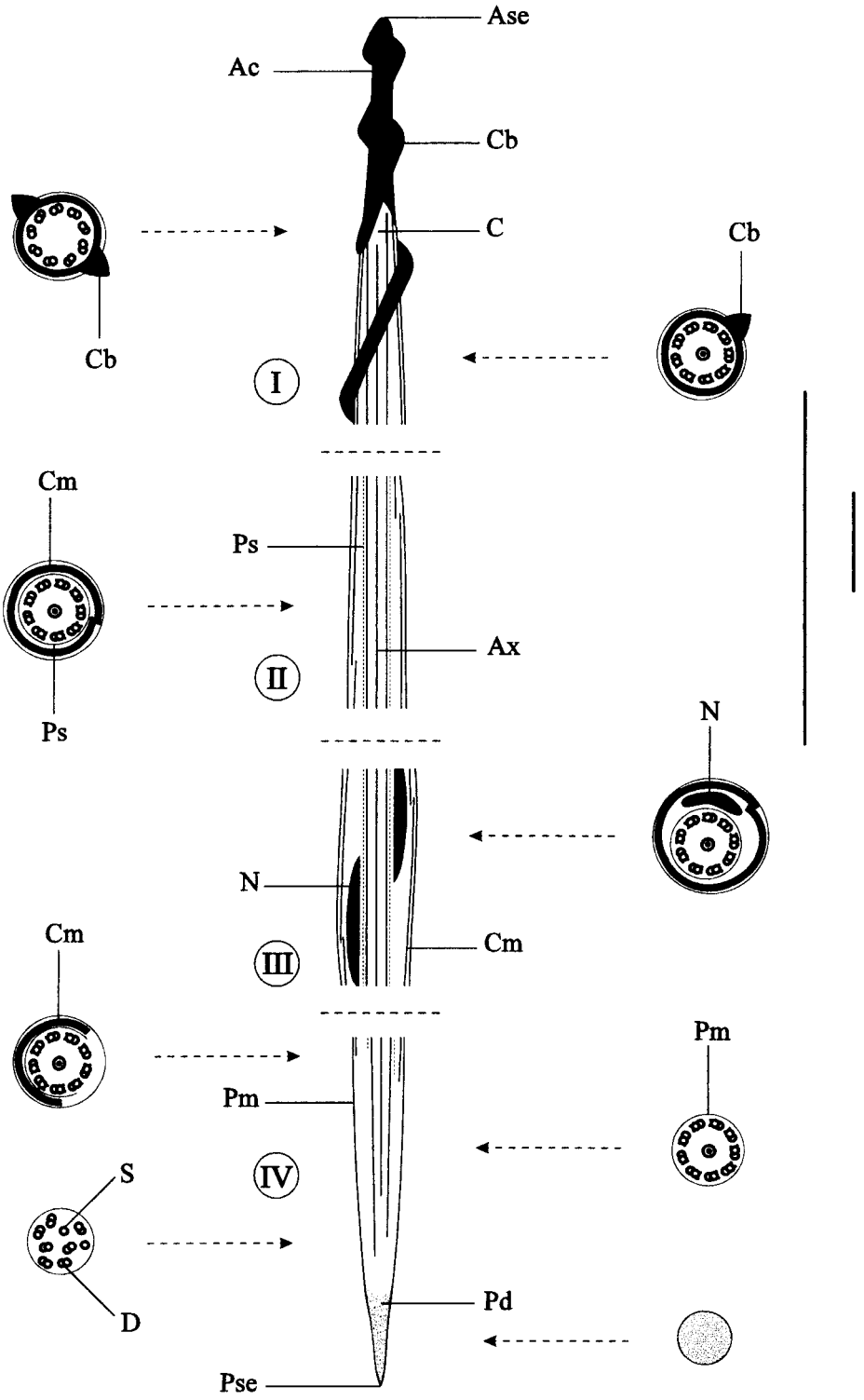

Fig. 21. Reconstruction of the spermatozoon in *Catenotaenia pusilla* possessing four regions (I–IV) from anterior to posterior. For clarity, the spiral coil of the cortical microtubules has not been shown. Ac, apical cone; Ase, anterior spermatozoon extremity; Ax, axoneme; C, centriole; Cb, crest-like bodies; Cm, cortical microtubules; D, doublets; N, nucleus; Pd, posterior electron-dense material; Pm, plasma membrane; Ps, periaxonemal sheath; Pse, posterior spermatozoon extremity; S, singlets. Bars = 1 μm (right bar for longitudinal sections and left bar for cross-sections).

It contains two centrioles, orthogonally disposed, and with neither associated striated roots nor an intercentriolar body between them (figs 1 and 20a). An axoneme develops on one of the centrioles (figs 2 and 20b), whereas the other remains oriented in a cytoplasmic bud and later aborts. The axoneme grows on the outside of the cytoplasmic extension (figs 2 and 20b). The angle between the axoneme and the cytoplasmic extension is about 45°. During the development of the axoneme the nucleus penetrates the spermatid body and cortical microtubules initiate its migration along the cytoplasmic extension (figs 2, 3 and 20c). Later, a flagellar rotation is produced and the nucleus migrates along the spermatid body (figs 3, 7 and 20c). A proximodistal fusion between the axoneme and the cytoplasmic extension is produced (figs 3, 4 and 20d). Posteriorly, two crest-like bodies appear in the anterior part of the spermatid and the nucleus completes its migration (figs 4, 5 and 20e). Finally, the ring of arched membranes narrows, strangulation is produced, and the mature spermatid detaches from the residual cytoplasm (figs 6, 8 and 20f).

Spermatozoon

In the spermatozoon of *C. pusilla* four regions from the anterior to posterior extremities were distinguished, with no clear morphological discontinuity between them, but where distinctive ultrastructural features could be observed.

Region I (figs 9, 10, 13, 14, 17 and 21) is about 325 nm wide and corresponds to the anterior extremity of the spermatozoon. It is capped by an apical cone of electron-dense material (1750 × 225 nm) (figs 9, 10 and 21). The axoneme, of the 9 + '1' pattern of the Trepaxonemata, is in a central position, surrounded by a thin layer of electron-lucent cytoplasm (figs 14 and 17). The submembranous cortical microtubules are spiralled at an angle of about 40° to the hypothetical spermatozoon axis and form a discontinuous layer (fig. 17). Externally, it exhibits two helical crest-like bodies spiralled at an angle of about 40° to the spermatozoon axis (figs 9, 10 and 21). These crest-like bodies are unequal in length and present a maximum thickness around 75 nm. One of these bodies completes its helical course around the spermatozoon at the level of the centriole or the initial portion of the axoneme (figs 10 and 17).

Region II (figs 11, 19 and 21) is around 400 nm wide. It lacks crest-like bodies but exhibits an axoneme surrounded by a periaxonemal sheath (figs 11 and 19), a thin layer of electron-lucent cytoplasm and a discontinuous layer of spiralled cortical microtubules (figs 11 and 19).

Region III (figs 12, 19 and 21) is the nuclear region and it measures about 450 nm in width. The nucleus is spiralled around the central axoneme and cross-sections reveal a kidney to horse-shoe shape (fig. 19).

Region IV (figs 15, 16, 18, 19 and 21) has a maximum width of about 300 nm. In this region cortical microtubules stop their helical course along the spermatozoon (fig. 19). The periaxonemal sheath also disappears at this level (fig. 19). Posteriorly, the axoneme becomes disorganized. The central core disappears, the peripheral doublets lose their arms, become disorganized and posteriorly transform into singlets (fig. 15). The posterior extremity of the spermatozoon is sharp and electron-lucent (figs 16 and 18).

Discussion

Catenotaenia pusilla shows a particular pattern of spermiogenesis not found previously in the Cyclophyllidea. It is a modification of the type III (according the classification of Bâ & Marchand, 1995), a spermiogenetic pattern described in diverse cyclophyllideans: *Mathevotaenia herpestis* (Anoplocephalidae), *Dipylidium caninum* (Dipylidiidae), *Raillietina tunetensis* (Hymenolepididae) and *Nematotaenia chantalae* (Nematotaeniidae) (Mokhtar-Maamouri & Azzouz-Draoui, 1990; Bâ & Marchand, 1994b,c; Miquel *et al.*, 1998). This pattern of spermiogenesis is characterized by the axoneme growing outside of the cytoplasmic extension and the absence of a flagellar rotation before the proximodistal fusion between the axoneme and the cytoplasmic extension. The absence of striated roots associated with the centrioles and the absence of an intercentriolar body between the two centrioles also characterize type III spermiogenesis. Nevertheless, in *C. pusilla* a flagellar rotation is observed. Other peculiarities of pattern III spermiogenesis are observed in other cyclophyllideans. This is the case for spermiogenesis in *D. caninum*, characterized by the presence of thin striated roots attached to each centriole (Miquel *et al.*, 1998). In fact, the absence of striated rootlets associated with centrioles is a feature postulated as a synapomorphy for the Cyclophyllidea and Tetrabothriidea (see Justine, 1998). However, *Anoplocephaloides dentata* is another cyclophyllid which presents thin striated roots in the spermatid (Miquel & Marchand, 1998a).

In the Cestoda, the presence of a helical crest-like body or bodies in the spermatozoon is a feature postulated as a synapomorphy by Bâ & Marchand (1995). The number of these structures varies from 1 to 12 and the Cyclophyllidea is the sole order within the Eucestoda which includes species with two crest-like bodies in the spermatozoon. The spermatozoon in *C. pusilla* shows two crest-like bodies. The other catenotaeniid studied, *S. lobata*, also presents two unequal crest-like bodies (Miquel *et al.*, 1997). For the remaining cyclophyllideans, two crest-like bodies have also been observed in some members of the family Anoplocephalidae (Bâ *et al.*, 1991; Bâ & Marchand, 1992a,1994d; Miquel & Marchand, 1998a,b) and in all members of the Davaineidae studied to date (Bâ & Marchand, 1994a,c).

In the Cyclophyllidea, the periaxonemal sheath has been suggested as a character for phylogenetic inference at the family level (Justine, 1998, 1999). At present, the Anoplocephalidae is the sole family in which this character is variable. Nevertheless, for the four subfamilies of anoplocephalids the case is clearly different. Thus, the Anoplocephalinae, Linstowiinae and Inermicapsiferinae show a single condition, i.e. the presence or absence of the periaxonemal sheath (MacKinnon & Burt, 1984; Bâ & Marchand, 1992a, 1994b,d,e; Miquel & Marchand, 1998a,b). In contrast, the Thysanosomatinae exhibits the presence and absence of the periaxonemal sheath depending on the different species studied (Bâ *et al.*, 1991; Bâ & Marchand, 1992b, 1994f). In the Catenotaeniidae, we described the presence of a periaxonemal sheath in the mature spermatozoon of *Skrjabinotaenia lobata*, a member of the subfamily Skrjabinotaeniinae (Miquel *et al.*, 1997).

Table 1. Ultrastructural features of spermiogenesis and the spermatozoon in *Skrjabinotaenia lobata* and *Catenotaenia pusilla*.

Spermatological data	*Skrjabinotaenia lobata* (Skrjabinotaeniinae) Miquel *et al*. (1997)	*Catenotaenia pusilla* (Catenotaeniinae) present paper
Spermiogenesis		
Type (according Bâ & Marchand, 1995)		III modified
Proximodistal fusion		+
Flagellar rotation		+
Angle of rotation		45°
Striated roots		–
Intercentriolar body		–
Spermatozoon		
Crest-like bodies		
Number	2	2
Maximum thickness*	60–80	75
Length	Unequal	Unequal
Apical cone (length×width)*	2500×200	1750×225
Cortical microtubules (angle)	40°	40°
Nucleus		
Morphology	Spiralled	Spiralled
Shape in cross-section	Kidney to horseshoe	Kidney to horseshoe
Dense granules	–	–
Periaxonemal sheath	+	+
Proteinaceus walls	–	–
Posterior extremity	Filiform	Sharp

+/–, presence/absence of considered characters; * measurements in nm.

On the other hand, our results match the polarity which exists between dense granules and the periaxonemal sheath. In this respect, Justine (1998) analyses the available data from different authors and determines a clear polarity between these two features. Thus, species with dense granules in the spermatozoon lack a periaxonemal sheath. The sole exception to date is the dipylidiid *D. caninum* which lacks granules and a periaxonemal sheath in its spermatozoon (Miquel & Marchand, 1997).

No clear differences have been observed in the ultrastructure of spermatozoa of *C. pusilla* and *S. lobata*. The most interesting ultrastructural features found in the mature spermatozoon in *C. pusilla* are also present in *S. lobata*. These features are the morphology of the apical cone, the number and morphology of crest-like bodies, the presence of a periaxonemal sheath and the end of cortical microtubules prior to the disorganization of the axoneme. Nevertheless, slight differences between them, such as length of the apical cone and the morphology of the posterior extremity of the spermatozoon have been observed (see table 1).

Acknowledgements

We would like to thank the 'Serveis Científics i Tècnics' of the University of Barcelona for their support in the preparation of material. This study was partially supported by the 'Comissionat per a Universitats i Recerca de la Generalitat de Catalunya' (1998-SGR-00003) and the DGICYT project PB 96–0401-CO2–01 of the 'Ministerio de Educación y Cultura' of Spain.

References

Bâ, C.T. & Marchand, B. (1992a) Ultrastructural study of the spermatozoa of *Moniezia expansa* Rudolphi, 1810 and *M. benedeni* Moniez, 1879 (Cestoda, Cyclophyllidea, Anoplocephalidae). *Annales de Parasitologie Humaine et Comparée* **67**, 111–115.

Bâ, C.T. & Marchand, B. (1992b) Ultrastructural particularities of the spermatozoon of *Stilesia globipunctata* (Cestoda) parasite of the small intestine of sheep and goats in Senegal. *Journal of Submicroscopic Cytology and Pathology* **24**, 29–34.

Bâ, C.T. & Marchand, B. (1994a) Similitude ultrastructurale des spermatozoïdes de quelques Cyclophyllidea. *Parasite* **1**, 51–55.

Bâ, C.T. & Marchand, B. (1994b) Ultrastructure of spermiogenesis and the spermatozoon of *Mathevotaenia herpestis* (Cestoda) intestinal parasite of *Atelerix albiventris* in Senegal. *Acta Zoologica (Stockholm)* **75**, 167–175.

Bâ, C.T. & Marchand, B. (1994c) Ultrastructure of spermiogenesis and the spermatozoon of *Raillietina (R.) tunetensis* (Cyclophyllidea, Davaineidae) intestinal parasite of turtle doves in Senegal. *International Journal for Parasitology* **24**, 237–248.

Bâ, C.T. & Marchand, B. (1994d) Comparative ultrastructure of the spermatozoa of *Inermicapsifer guineensis* and *I. madagascariensis* (Cestoda, Anoplocephalidae, Inermicapsiferinae) intestinal parasites of rodents in Senegal. *Canadian Journal of Zoology* **72**, 1633–1638.

Bâ, C.T. & Marchand, B. (1994e) Ultrastructure of spermiogenesis and the spermatozoon of *Aporina delafondi* (Cyclophyllidea, Anoplocephalidae) intestinal parasite

of turtle doves in Senegal. *International Journal for Parasitology* **24**, 225–235.

Bâ, C.T. & Marchand, B. (1994f) Ultrastructure of the spermatozoon of *Avitellina centripunctata* (Cestoda, Cyclophyllidea), a parasite of the small intestine of cattle in Senegal. *Acta Zoologica (Stockholm)* **75**, 161–166.

Bâ, C.T. & Marchand, B. (1995) Spermiogenesis, spermatozoa and phyletic affinities in the Cestoda. pp. 87–95 *in* Jamieson, B.G.M., Ausió, J. & Justine, J.-L. (*Eds*) *Advances in spermatozoal phylogeny and taxonomy. Mémoires du Muséum national d'Histoire naturelle (Paris)* **166**. Éditions du Muséum national d'Histoire naturelle, Paris.

Bâ, C.T. & Marchand, B. (1998) Ultrastructure of spermiogenesis and the spermatozoon of *Vampirolepis microstoma* (Cestoda, Hymenolepididae), intestinal parasite of *Rattus rattus*. *Microscopy Research and Technique* **42**, 218–225.

Bâ, C.T., Marchand, B. & Mattei, X. (1991) Demonstration of the orientation of the Cestoda spermatozoon illustrated by the ultrastructural study of spermiogenesis and the spermatozoon of a Cyclophyllidea: *Thysaniezia ovilla* Rivolta, 1874. *Journal of Submicroscopic Cytology and Pathology* **23**, 605–612.

Justine, J.-L. (1995) Spermatozoal ultrastructure and phylogeny of the parasitic Platyhelminthes. pp. 55–86 *in* Jamieson B.G.M., Ausió, J. & Justine, J.-L. (*Eds*) *Advances in spermatozoal phylogeny and taxonomy. Mémoires du Muséum national d'Histoire naturelle (Paris)* **166**. Éditions du Muséum national d'Histoire naturelle, Paris.

Justine, J.-L. (1998) Spermatozoa as phylogenetic characters for the Eucestoda. *Journal of Parasitology* **84**, 385–408.

Justine, J.-L. (1999) Spermatozoa of Platyhelminthes: comparative ultrastructure, tubulin immunocytochemistry and nuclear labeling. pp. 1–12 *in* Gagnon, C. (*Ed.*) *The male gamete: from basic knowledge to clinical applications.* Vienna, Illinois, Cache River Press.

MacKinnon, B.M. & Burt, M.D.B. (1984) The comparative ultrastructure of spermatozoa from *Bothrimonus sturionis* Duv. 1842 (Pseudophyllidea), *Pseudanthobothrium hanseni* Baer, 1956 (Tetraphyllidea) and *Monoecocestus americanus* Stiles, 1895 (Cyclophyllidea). *Canadian Journal of Zoology* **62**, 1059–1066.

Miquel, J. & Marchand, B. (1997) Ultrastructure of the spermatozoon of *Dipylidium caninum* (Cestoda, Cyclophyllidea, Dilepididae), intestinal parasite of *Canis familiaris*. *Parasitology Research* **83**, 349–355.

Miquel, J. & Marchand, B. (1998a) Ultrastructure of spermiogenesis and the spermatozoon of *Anoplocephaloides dentata* (Cyclophyllidea, Anoplocephalidae), intestinal parasite of Arvicolidae rodents. *Journal of Parasitology* **84**, 1128–1136.

Miquel, J. & Marchand, B. (1998b) Ultrastructure of the spermatozoon of the bank vole tapeworm, *Paranoplocephala omphalodes* (Cestoda, Cyclophyllidea, Anoplocephalidae). *Parasitology Research* **84**, 239–245.

Miquel, J., Bâ, C.T. & Marchand, B. (1997) Ultrastructure of the spermatozoon of *Skrjabinotaenia lobata* (Cyclophyllidea, Catenotaeniidae), intestinal parasite of *Apodemus sylvaticus* (Rodentia, Muridae). *Journal of Submicroscopic Cytology and Pathology* **29**, 521–526.

Miquel, J., Bâ, C.T. & Marchand, B. (1998) Ultrastructure of spermiogenesis of *Dipylidium caninum* (Cestoda, Cyclophyllidea, Dipylidiidae), an intestinal parasite of *Canis familiaris*. *International Journal for Parasitology* **28**, 1453–1458.

Miquel, J., Feliu, C. & Marchand, B. (1999) Ultrastructure of spermiogenesis and the spermatozoon of *Mesocestoides litteratus* (Cestoda, Mesocestoididae). *International Journal for Parasitology* **29**, 499–510.

Mokhtar-Maamouri, F. & Azzouz-Draoui, N. (1990) Étude de la spermiogénèse et de l'ultrastructure du spermatozoïde de *Nematotaenia chantalae* Dollfus, 1957 (Cestoda, Cyclophyllidea, Nematotaeniidae). *Annales de Parasitologie Humaine et Comparée* **65**, 221–228.

Reynolds, E.S. (1963) The use of lead citrate at high pH as an electron-opaque stain in electron microscopy. *Journal of Cell Biology* **17**, 208–212.

Sène, A., Bâ, C.T. & Marchand, B. (1999) Ultrastructure of spermiogenesis of *Phyllobothrium lactuca* (Cestoda, Tetraphyllidea, Phyllobothriidae). *Folia Parasitologica*, in press.

Swiderski, Z. (1970) An electron microscope study of spermatogenesis in cyclophyllidean cestodes with emphasis on the comparison of fine structure of mature spermatozoa. *Journal of Parasitology* **56**, 337.

Thiéry, J.P. (1967) Mise en évidence des polysaccharides sur coupes fines en microscopie électronique. *Journal of Microscopy* **6**, 987–1018.

(Accepted 19 May 1999)